THE DISTRIBUTION OF RADIO BRIGHTNESS OVER THE SOLAR DISK AT A WAVELENGTH OF 21 CENTIMETRES

III. THE QUIET SUN—TWO-DIMENSIONAL OBSERVATIONS

By W. N. Christiansen* and J. A. Warburton*

[*Manuscript received July* 25, 1955]

Summary

A distribution of solar radio brightness at a wavelength of 21 cm has been derived from observations made during the period of low sunspot activity from 1952 to 1954. The observations were made using two multiple interferometers arranged at right angles; this enabled the solar disk to be scanned in many different directions. The derived one-dimensional profiles of the quiet Sun for these various scanning directions were combined and a Fourier method adopted to derive a two-dimensional brightness distribution. The distribution shows marked limb-brightening in the equatorial zones but none in the polar regions. The contours of brightness are in general conformity with those expected from a solar atmosphere having a coronal electron density distribution of the kind proposed by van de Hulst for the period of minimum sunspot activity.

I. Introduction

It has been established in the past few years that solar radiation at decimetre wavelengths has an essentially steady background component. This "quiet" solar component has been the subject of much study recently in efforts to determine distributions of brightness across the solar disk, and work has been carried out at many radio wavelengths in the range from 6 cm to about 8 m. One of these studies was made at a wavelength of 21 cm using an aerial system which has been described in Part I of this series (Christiansen and Warburton 1953*a*). However, an essential limitation of this fixed aerial system was that the solar disk was scanned in a more or less fixed direction in a strip-wise manner by the aerial beam; consequently it was necessary to assume that the Sun had certain symmetry in order to solve the brightness distribution problem. This work, which has been described as a one-dimensional study, forms the subject matter of Part II of the series (Christiansen and Warburton 1953*b*). The presence of limb-brightening was an outstanding feature of the brightness distribution published.

In the absence of contrary information, the simplifying assumption was made that the solar disk shows circular symmetry when observed at a wavelength of 21 cm. Visual observations of the solar corona during eclipses at times of sunspot minimum have suggested that this assumption is probably not correct. In addition, radio observations during solar eclipses by Denisse, Blum, and Steinberg (1952) have given evidence of departure from circular symmetry

* Division of Radiophysics, C.S.I.R.O., University Grounds, Sydney.

RADIO BRIGHTNESS OVER THE SOLAR DISK. III

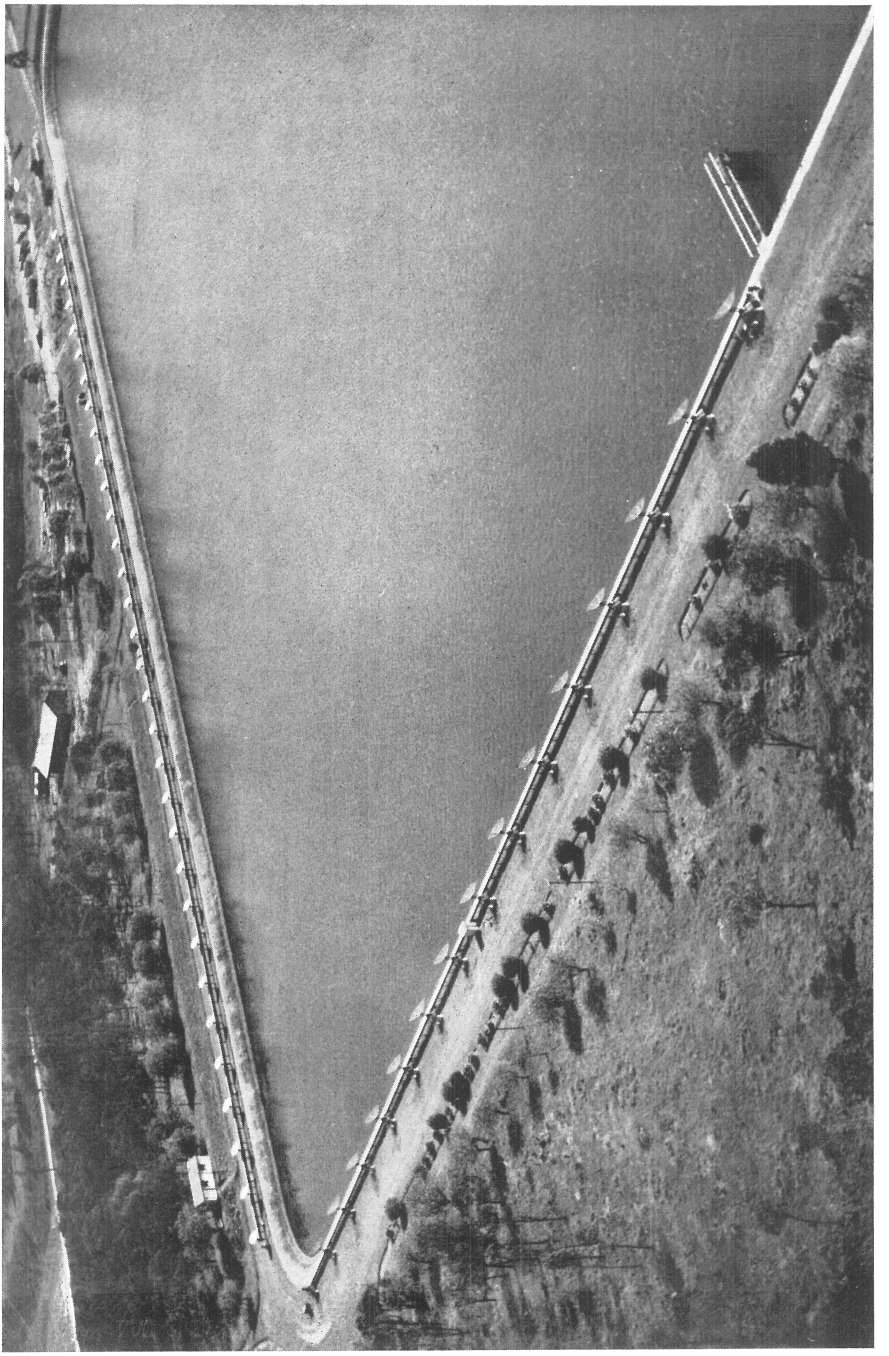

Aerial photograph of the two multiple interferometers.

RADIO BRIGHTNESS OVER THE SOLAR DISK. III

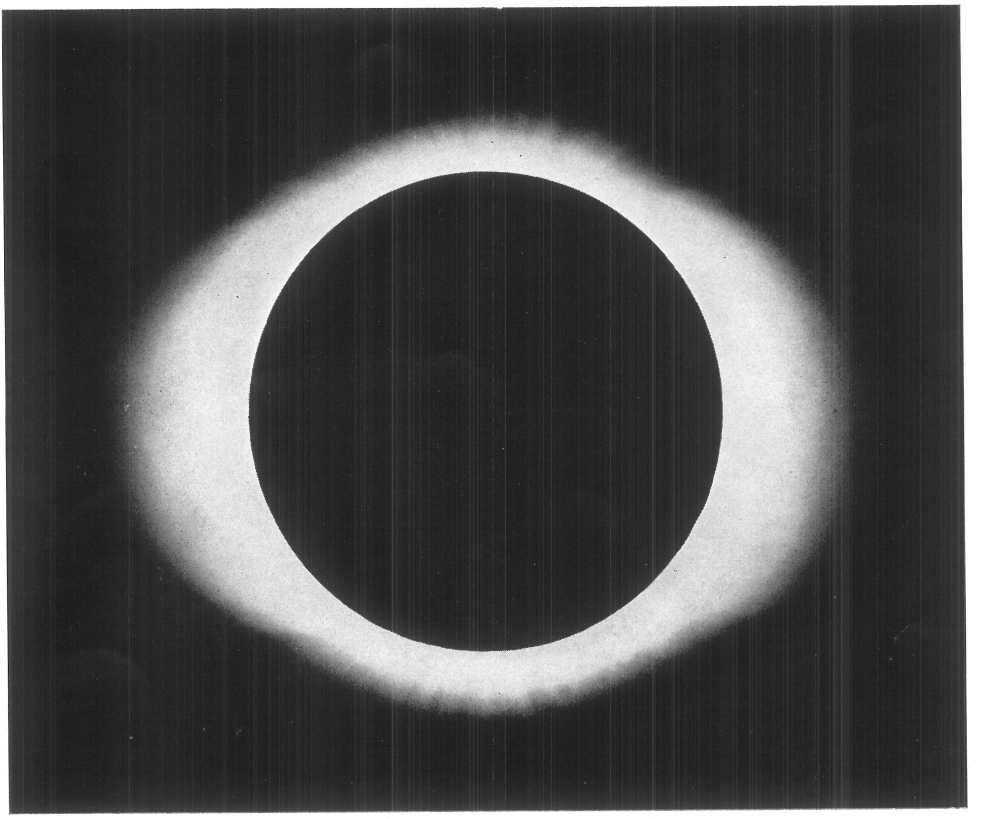

Photograph of the Sun at the total eclipse June 30, 1954 (M. Waldmeier).

of the solar disk at a wavelength of 1·78 m. The early observations at a wavelength of 21 cm by the present authors had also shown that the apparent width of the Sun seemed to change as the scanning direction varied with respect to the direction of the Sun's axis.

With the previous equipment it was not possible to scan the Sun in directions that differed greatly from the direction along the solar equator. A new multiple interferometer was built, therefore, in a direction at right angles to the earlier one. By use of the two interferometers it was possible to scan the Sun over a great variety of angles during the course of a day, and at practically any desired angle over the course of several months. From these one-dimensional scans it has been possible to reconstruct a two-dimensional brightness distribution (smoothed by the aerial) by a method of Fourier analysis.

A preliminary report of this work was given at the XIth General Assembly of U.R.S.I. where, at the same time, complementary results at a wavelength of 60 cm were reported from Cambridge. These two-dimensional results, together with those already published by O'Brien (1953) at 1·4 m wavelength, all show that the source is not circular. They also exhibit distinct differences in the degree of limb-brightening, particularly in the equatorial regions of the Sun; the maximum degree of brightening occurs at the shortest wavelength, 21 cm. The most outstanding feature of the two-dimensional distribution at 21 cm is the restricted zones in which limb-brightening is observed. No such brightening occurs in the polar regions of the sun; this is confined to the equatorial zone.

II. Equipment

The complete equipment used consisted of a grating-type interferometer of 32 equally spaced elements (described in Part I of this series) aligned approximately east-west, and a similar 16-element system arranged in an approximately north-south direction (see Plate 1). Each system has its own receiver, and all the elements of each system are connected to the receiver through equal lengths of cable. If d is the distance between adjacent elements and ψ the angle between the normal to the line of the aerials and the direction of a ray arriving at the aerial, then the angles of maximum response are given by $\sin \psi = n\lambda/d$, where n is an integer and λ the wavelength. The locus of a point making a constant angle ψ with the normal to the aerial is a small circle on the celestial sphere with the line of the aerials as axis (see Fig. 1). These small circles give the positions on the celestial sphere at which the aerial has a maximum response. If now we consider the daily motion of the Sun through such a system of beams we see (Fig. 2)* that the direction in which the Sun is scanned by the strip beams varies throughout the day. The observations on the east-west aerial were confined to a period around the hour angle (H.A.) 348°, or 12° east. Near this time the inclination of the aerial "beams" to the Sun's central meridian remains fairly constant; hence an almost exact repetition of the

* Figure 2 shows a section of a sphere on which two systems of small circles have been drawn representing the positions of the aerial beams. This sphere was used as an aid in quick analysis of the records.

pattern is produced as successive beams scan the disk. A typical record shows this (Fig. 3 (*a*)). With the beams produced by the north-south system, however, the observations were made from about H.A. 320° (i.e. 40° east) to H.A. 30°.

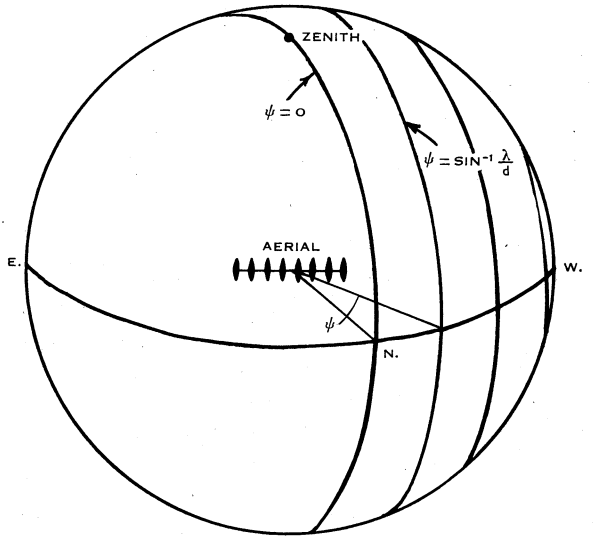

Fig. 1.—Loci of points of maximum response of a multiple interferometer as used in this work.

During this period the scanning angle changes through a range of about 50°. As the angle changes, so does the rate at which the solar disk passes through the beam. This feature is depicted clearly in the reproduced record (Fig. 3 (*b*)).

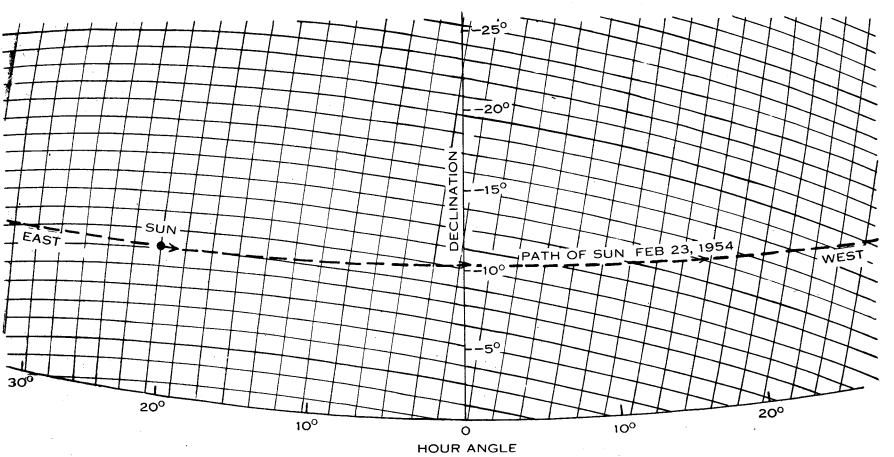

Fig. 2.—Path of the Sun through the two systems of aerial beams on one day.

Each of the aerial systems produces directly one-dimensional power *v*. time diagrams. From a knowledge of the Sun's declination the time coordinate is readily converted to the angular separation θ between the aerial beam (scanning

strip) and the centre of the optical disk. The overall length of the east-west aerial is 1028 wavelengths producing beams around midday of 3 min of arc width, while the north-south aerial of 760 wavelengths produces beams, for small values of ψ, of about 4 min of arc width. The beams actually used in the latter system depend on the Sun's declination, and for the period of observations their width ranged from 4 to nearly 5 min of arc.

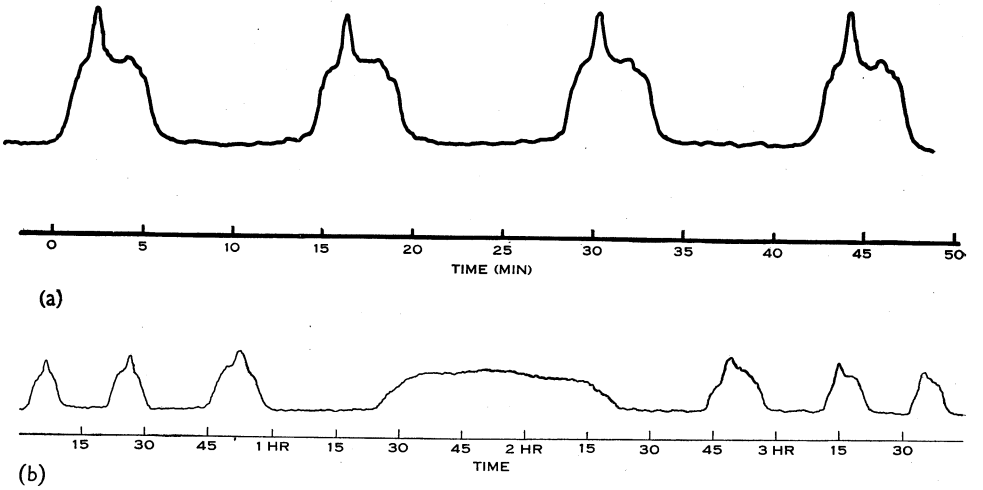

Fig. 3.—Typical daily records of the passage of the Sun through several aerial beams, (*a*) using the east-west interferometer, (*b*) using the north-south interferometer.

III. Observations

A series of observations has been made using both aerial systems over the period September 1953 to April 1954. We have also made observations from April 1952 to September 1953 using the east-west aerial system alone. The combination of these observations over such a long period to solve the distribution is considered to be valid because no changes in the shape or extent of the quiet Sun were detected during the period 1952–1954, for the scanning directions φ lying between 55° and 90°. Figure 4 shows two quiet-Sun curves observed at the same scanning angle in 1952 and 1954. Any differences are within the experimental errors.

During the observations with the two independent systems it has been possible on any one day to scan the Sun in many different directions. A typical result for October 15, 1953 is reproduced in Figure 5, where the effect of scanning the Sun in two directions differing by 68° is shown. The departure from circular symmetry of the quiet Sun is clearly illustrated by these observations.

By making use of the seasonal variation of the Sun's orientation with respect to the two sets of aerial beams, it has been possible to obtain records covering 140° out of 180° range of scanning angle, as indicated in Figure 6. (The scanning angle φ is defined as the angle between the Sun's central meridian and the normal to the aerial beam.)

The geometry of the two systems is such that the range of angles covered by one system is complementary to that of the other, the two ranges approaching to within 6° of one another. Obviously, the time taken for the Sun to drift

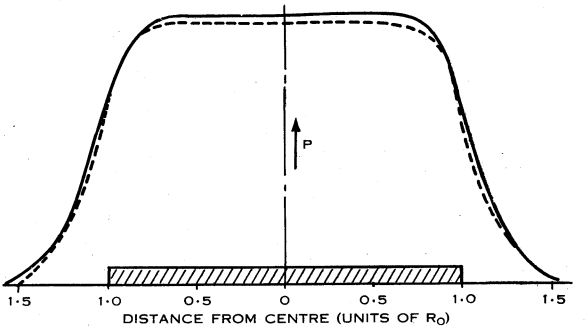

Fig. 4.—One-dimensional quiet Sun profiles for the same scanning direction $\varphi=58°$. ---- 1952, —— 1954. P is the power received in arbitrary units.

through a beam depends on its declination, on the angle that the beam makes with the Sun's diurnal path, and on the Sun's semi-diameter. It is therefore

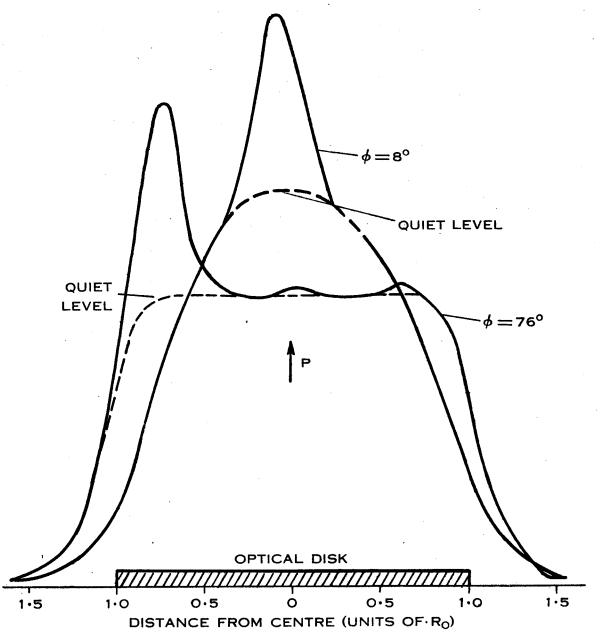

Fig. 5.—One-dimensional profiles showing the result of scanning the Sun in different directions on the same day.

necessary to normalize the time scale of each record. The next step is to subtract contributions due to localized bright regions. For this purpose we superposed several diagrams, taken on different days for each scanning direction, and drew

the lower envelope (see Part II). Figure 7 shows the result of superimposing several days' observations for an average scanning angle of 28°. The deduction

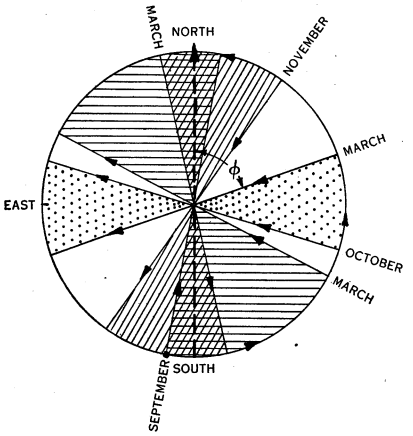

SHADING	INTERFEROMETER USED	OBSERVATION PERIOD (LOCAL TIME)
	N.— S.	0800 → 1200 HR
	E.— W.	1000 → 1200 HR
	N.— S.	1200 → 1500 HR

Fig. 6.—Range of scanning angles φ covered by the two aerial systems.

of the quiet Sun level from such superimposed diagrams was usually not very difficult because during the period of observation localized regions of enhanced brightness on the Sun were not frequent.

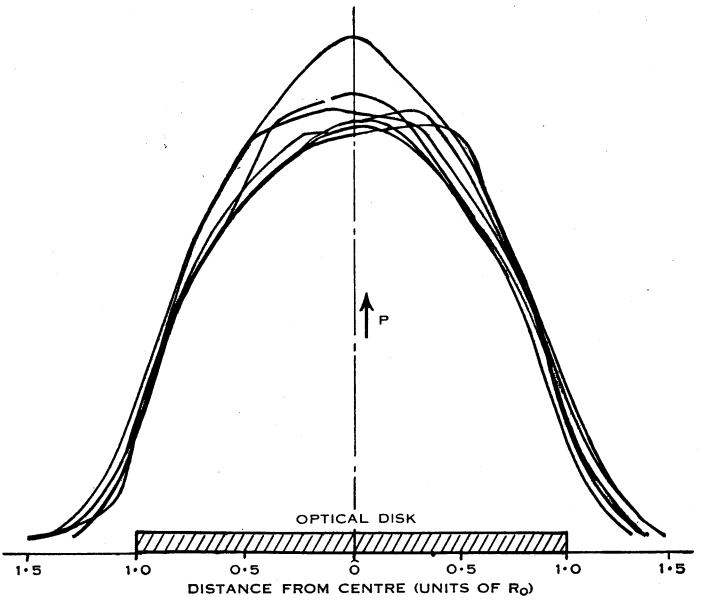

Fig. 7.—A succession of daily records for scanning directions near $\varphi=28°$ superimposed to show the contribution of the quiet Sun.

Now, each of the one-dimensional curves is symmetrical; also the same result is obtained for each direction which makes the same given angle with the Sun's central meridian. Such observations indicate that the true brightness

distribution should possess quadrant symmetry. For this reason we have restricted the analysis to one quadrant of the distribution, $\varphi=0°$ to $\varphi=90°$. Figure 8 shows the set of observed one-dimensional scans used in the analysis. These are for angles of $\varphi=0$, 28, 42, 51, 57, 69, and 82°, and each is the average curve over a range of angles of $\varphi\pm6°$. These scans represent the one-dimensional or line integrated brightness distributions over the solar disk, smoothed by the effect of the aerial beam.

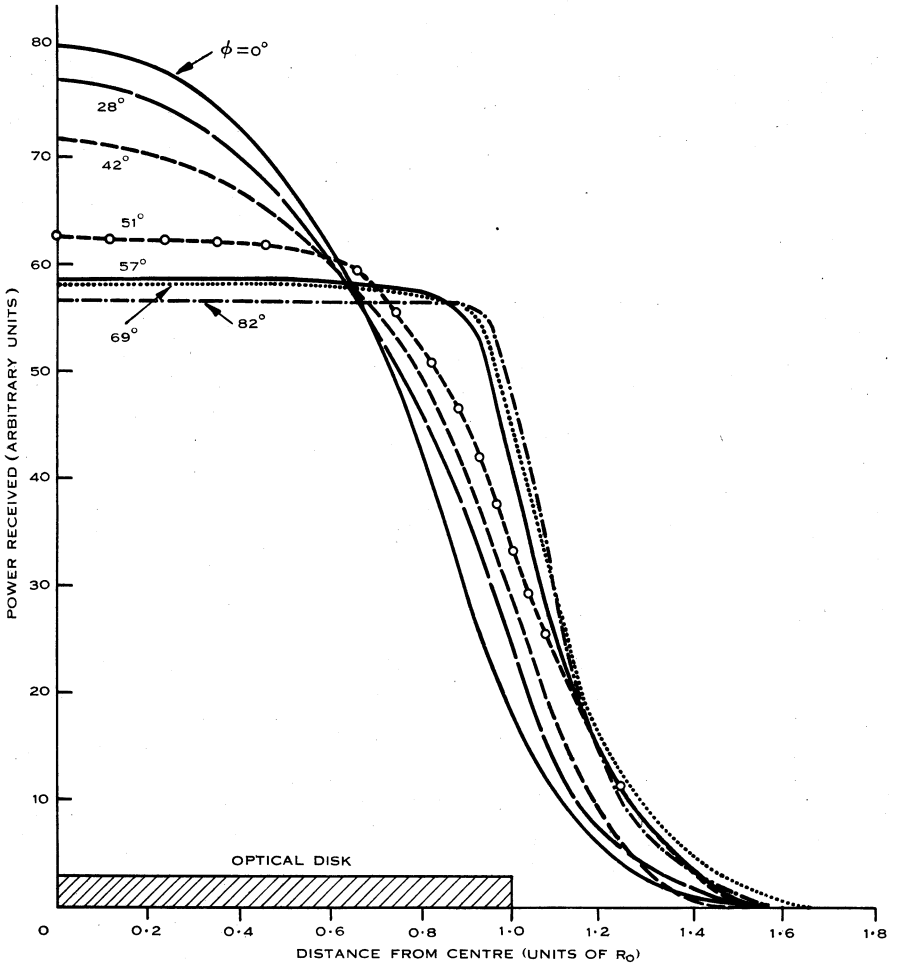

Fig. 8.—One-dimensional quiet Sun profiles used in the analysis for several scanning angles φ.

IV. The Derivation of the Brightness Distribution from the Observations by a Method of Fourier Analysis

The way in which a two-dimensional radio brightness distribution may be derived from a number of one-dimensional scans is not obvious. However, rather similar two-dimensional problems have arisen in the field of crystallography, and solutions for these problems, using the methods of Fourier analysis,

have been found. Such a method of solution has been applied to the problem of a radio brightness distribution by O'Brien (1953). It is well known that the two-aerial interferometer, as used by O'Brien and others, measures the Fourier components of the strip integration of the real distribution, and that the frequency of the component being observed is determined by the aerial spacing. With a grating-type interferometer, as used in this work, the one-dimensional distribution is observed directly. The Fourier component of highest frequency contained in the distribution is of course determined by the length of the aerial system. Hence, if we take the Fourier transform of this one-dimensional distribution, the available information is then in a similar form to that of O'Brien and the subsequent solution of the two problems becomes identical. A full discussion of this problem is in preparation by Smerd and Wild.

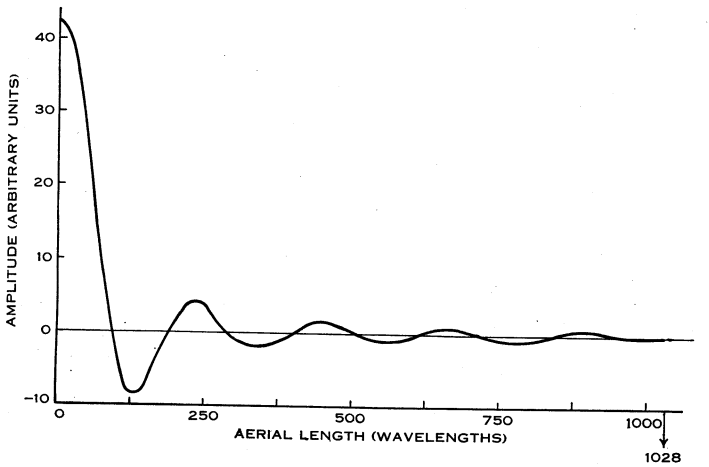

Fig. 9.—Cosine Fourier transform of the one-dimensional profile of the quiet Sun in the direction $\varphi = 75°$.

The procedure adopted in the derivation of the two-dimensional distribution was as follows. The cosine Fourier transform of each one-dimensional distribution was first determined numerically. Only the even (cosine) terms of the Fourier components are present because each of the observed distributions is symmetrical. A typical cosine transform of one of the observed distributions is shown in Figure 9, and it is seen that both positive and negative values appear. Each of these transforms has a finite high frequency cut-off which is inversely proportional to the width of the aerial beam used in the observation. Since it seemed undesirable in the analysis to have higher resolution in some directions than in others (the beam widths varied from less than 3 min of arc to slightly more than 4 min of arc), some transforms have been degraded so that all correspond to the use of a uniformly fed aperture aerial with a half-power beam width of 4·3 min of arc. By plotting each of these "rippled" transforms radially in the direction corresponding to its scanning direction, a two-dimensional Fourier transform diagram was constructed. Contours of equal amplitude were drawn. The amplitude at the centre of the diagram, being the zero-frequency

component, is of course given by the area under the one-dimensional distribution curves and is the same for each curve. We now strip integrate this diagram, the strip summations being perpendicular to the scanning directions. The cosine Fourier transforms of these strip integrals give the radial cross sections of the brightness distribution in their corresponding scanning directions. The two-dimensional distribution is then obtained directly by plotting these radial cross sections and drawing contours of equal brightness. Figure 10 shows the derived

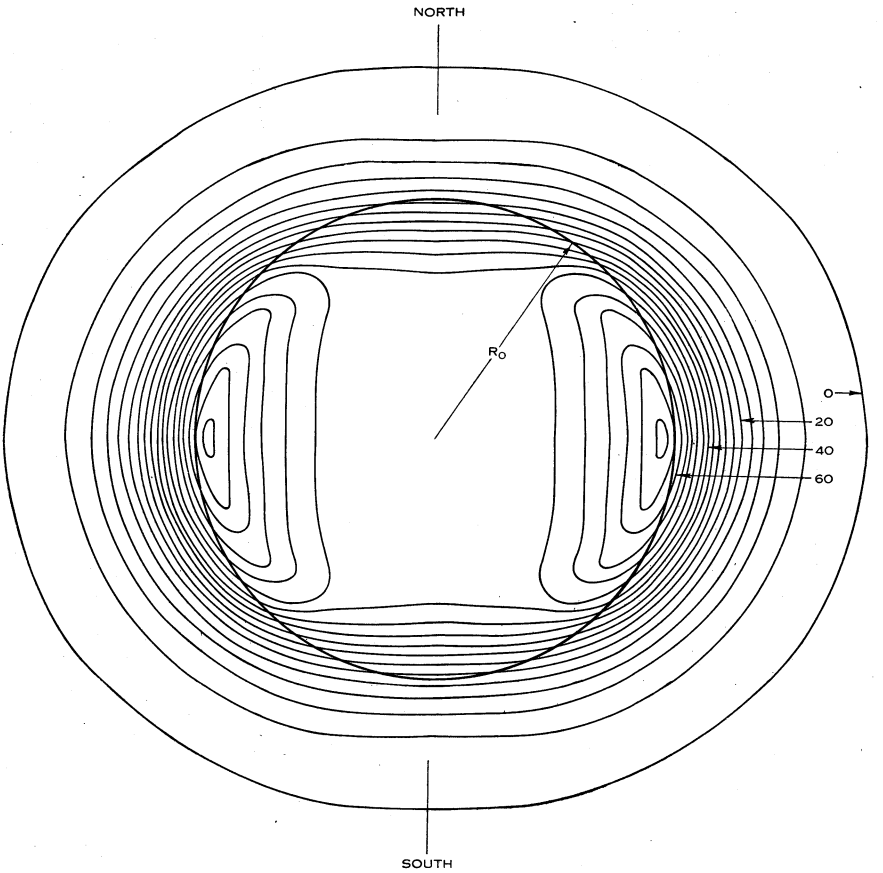

Fig. 10.—Derived two-dimensional radio brightness distribution. The contours are at equal intervals of 4×10^3 °K. The central brightness temperature is $4\cdot7\times10^4$ °K, and the maximum peak brightness is $6\cdot8\times10^4$ °K.

distribution. In the absence of errors in the calculations, line integration of the distribution in Figure 10 should reproduce the observed one-dimensional curves in Figure 8. In fact this process produces curves which differ from those in Figure 8 by less than 3 per cent. at any point.

If we know the total flux received from the quiet Sun, it is possible to assign absolute magnitudes of brightness temperature to the contours of Figure 10. For this, the apparent disk temperature (T_d) of the quiet Sun was taken as $7\cdot0\times10^4$ °K. This temperature was deduced from the lowest limits of solar

radio frequency flux as published in the I.A.U. Quarterly Bulletin of Solar Activity. During 1953, the lowest limits of flux coincided with the complete absence of local bright regions on the solar disk as seen on our records, and hence these values may be taken to refer to the quiet Sun.

V. The Distribution: Features

The most outstanding feature of the distribution is the departure from circular symmetry. This characteristic has been found elsewhere at lower frequencies. Eclipse observations by Denisse, Blum, and Steinberg (1952) at 169 Mc/s were interpreted to demonstrate marked departure from a circularly symmetrical source. The source was shown to extend 1·6 times further in the equatorial direction than in the direction of the solar axis. More recently O'Brien (1953), from observations at 1·4 m, has given a two-dimensional distribution which extends 1·2 times further along the equatorial direction than in the direction of the solar axis. The lower contours of the distribution in Figure 10 also show this feature. If we choose the contour at which the brightness temperature has fallen to half the centre value, then the radial extent is 1·25 R_0 in the equatorial direction, whereas it is 0·94 R_0 in the direction of the poles.

The contours of Figure 10 are at equal intervals of brightness temperature $T_b = 4 \cdot 0 \times 10^3$ °K, the brightness temperature at the centre being $4 \cdot 7 \times 10^4$ °K.

The limb-brightening reported in Part I is found to be confined to the equatorial regions. The peak of brightness appears to fall just inside the optical limb, rather than just beyond, as predicted theoretically. This discrepancy may not be significant, however, as the effect of the aerial beam has not been removed, and it is readily seen that smoothing by the aerial beam could cause the peak to fall inside its true position. The value of the peak in the derived brightness temperature is 1·46 times the value at the centre, i.e. $6 \cdot 8 \times 10^4$ °K, and falls off to 1·2 times in a direction 60° from the pole. At angles less than 30° no limb brightening occurs at all (see Fig. 11). Another effect of the aerial beam, which has been pointed out in Part II, is to make the real values for the peak brightness indeterminate. Hence the true brightness temperatures at the optical limb may be considerably higher than the values quoted.

The heliographic latitude at which limb-brightening ends is about 55°, which is approximately the latitude at which changes in the coronal structure can be seen at times of sunspot minimum. This feature is shown very clearly in the remarkable photograph (Plate 2) of the solar corona obtained by Waldmeier* during the eclipse of June 1954. At this time the sunspot activity cycle was in its minimum phase, and the Sun was exceptionally free from active regions; hence the photograph is very well suited for comparison with the derived quiet Sun distribution. The photograph shows that the structure and extent of the corona change at latitudes around 50° to 60°; at latitudes higher than these, polar plumes appear, while near the equator the corona extends to form well-defined wings. The corresponding feature at the 55° latitude in the derived

* We are indebted to Professor M. Waldmeier for permission to reproduce this photograph.

brightness distribution (Fig. 10) is the change from limb-brightening to limb-darkening.

The greater radial extent in the equatorial direction compared with that in the direction of the poles is also evident in the photograph. This feature can be compared in more detail with the radio brightness distribution, since the photographic image shows an apparent limit to the corona, and this limit is, in fact, a brightness contour for the corona. If we compare this contour with those of Figure 10, we find that the 8000 °K contour follows closely the outline of the corona as it appears in the photograph. (The " kinks " in the optical picture would not be expected to appear in the radio picture because of the

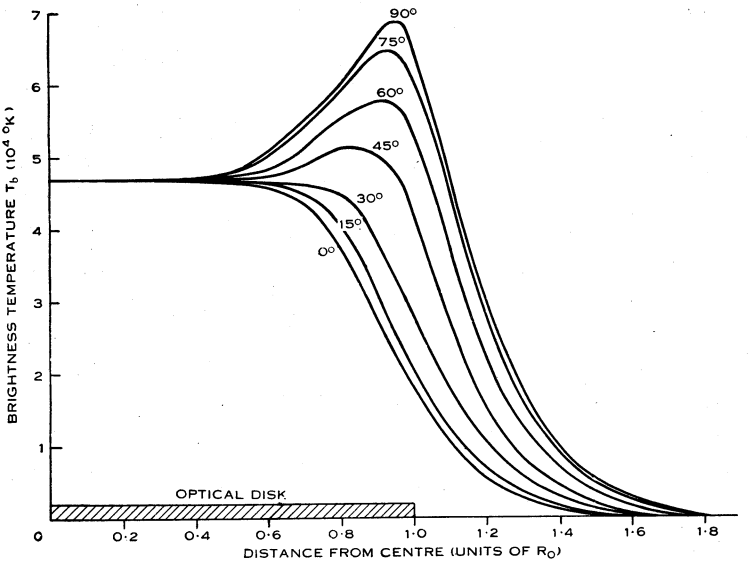

Fig. 11.—Derived radial brightness distributions in several directions with respect to the pole of the Sun.

smoothing effect of the radio aerial.) In both cases the part of the solar corona that is depicted is optically thin. This means that the contours represent lines of constant numbers of electrons integrated along the line of sight in the optical case, and (assuming uniform coronal temperature) constant means of the square of this number over regions around the line of sight in the radio case. The agreement between radio and optical contours (within the limitations imposed by the smaller resolution of the radio telescope) is satisfactory. It highlights the complementary nature of radio and optical studies of the Sun, and it may be taken as substantiating prevailing ideas on the origin of quiet Sun radiation at centimetre wavelengths.

VI. The Distribution : Discussion

It is generally agreed that at decimetre wavelengths pronounced limb-brightening is likely to occur because of the large increase in the coronal contribution to the radiation at the limb compared with that at the centre of the disk.

The radiation in the centre emanates mainly from the chromosphere. This is because the opacity of the corona in the line of sight is relatively small. Near the limb, however, the emergent ray is confined to the corona and, because the ray path in this region is longer, the opacity is greater. Since the electron temperature of the corona is much higher than that of the chromosphere, the brightness temperature observed in these regions may be higher.

In the two-dimensional distribution presented in Figure 10 this brightening occurs in the equatorial region, the degree of brightness and the position at which it occurs conforming qualitatively with the values predicted theoretically from simple solar models.

The observed brightness distribution, by itself, cannot be used to derive the distribution of temperature and pressure anywhere in the solar atmosphere. Even if similar information at other radio frequencies is available, it appears that a determination of these quantities requires the addition of information from optical solar observations. One procedure that can be adopted is to postulate model solar atmospheres which are consistent with what is known from optical observations and to compare the theoretical brightness distributions from such sources with that derived from observation. This comparison, however, is not usually direct. It must be remembered that the observations have been made with an aerial system of some particular resolving power, and unresolved features in the emitting surface of the Sun cannot be reproduced from the observations. Near the limb of the Sun's disk, where rapid changes in brightness with radial distance may occur, smoothing by the aerial system may be expected, and observed peak values of brightness temperature may fall well below the true values. A comparison between observed and theoretical brightness distributions should therefore be made using distributions which have been smoothed to the same extent.

In this paper we shall not attempt a detailed comparison between the observed and theoretical brightness distributions; we shall simply indicate that the brightness temperatures derived from the observations, and the temperatures expected from simple models based on available optical and radio data, are not grossly at variance.

For the appropriate period, that is, of sunspot minimum, the only values available for the electron density in the Sun's corona are those of van de Hulst (1949), who has tabulated the densities for both the equatorial and polar regions of the corona. If we employ these values in a simple solar model in which a uniform temperature corona is assumed, and consider two points at a radius of $1 \cdot 05$ times the optical radius of the Sun where only coronal emission will be observed, we find that, for a 10^6 °K corona, the brightness temperature at the equator would be $5 \cdot 7 \times 10^4$ °K and at the pole, $2 \cdot 0 \times 10^4$ °K.* These values are in order of magnitude agreement with those of $4 \cdot 7 \times 10^4$ °K and $1 \cdot 4 \times 10^4$ °K derived from our observations.

The derived brightness temperature for the central ray is of importance because in this region one may expect that the finite beam width of the aerial

* The authors wish to thank Mr. S. F. Smerd for some of his unpublished computations which were used in these calculations.

will produce little error in the measurement. If we use the same model corona as before, we find that about 15 per cent. of the radiation in the central ray originates in the corona. Hence the chromospheric component has an effective brightness temperature of 4×10^4 °K. To relate this value with electron temperatures and pressures in the chromosphere one may combine the result with those at other frequencies and also with the results of optical observations, as was done, for example, by Piddington (1954).

(*a*) *Long-term Variations in the Quiet Sun*

The radio-frequency brightness distribution in Figure 10 has been obtained from observations made at or near to a minimum of the sunspot cycle. As the region of origin of radiation at this wavelength lies partly in the corona, it is possible that the brightness distribution may change with the solar cycle as visual observations of the corona strongly suggest. Evidence of changes in the radio emission from the quiet Sun during the solar cycle was found by Covington (1949) and Christiansen and Hindman (1951). However, the latter results have been challenged by Piddington and Davies (1953), who consider that previous estimates of the quiet Sun radiation, made during sunspot maximum, actually involved a considerable proportion of radiation from old active regions on the Sun. They conclude that there has been no significant change in the output of the quiet Sun. Further measurements of the radio brightness distribution at other times in the solar cycle are obviously needed to resolve the problem of whether the quiet Sun does or does not change during the sunspot cycle.

VII. Conclusions

The measurements of brightness distributions at a wavelength of 21 cm have shown that at sunspot minimum the brightness shows differences between equatorial and polar regions which agree qualitatively with the eclipse photographs of the Sun at sunspot minimum. Further measurements will be required to determine whether there are significant changes in the brightness distribution during the course of a solar cycle. From visual observations this would be expected, and we must wait until the cycle moves away from its minimum phase before we can verify the changes which have been predicted.

VIII. Acknowledgments

The authors wish to acknowledge the help of Mr. G. Swarup in the computations involved in this work, and of Mr. G. Chandler and Mr. C. Fryar in the taking of the observations. We wish to thank also Mr. J. P. Wild and Mr. S. F. Smerd for their helpful criticism of the paper.

IX. References

Christiansen, W. N., and Hindman, J. V. (1951).—*Nature* **167** : 635.
Christiansen, W. N., and Warburton, J. A. (1953*a*).—*Aust. J. Phys.* **6** : 190.
Christiansen, W. N., and Warburton, J. A. (1953*b*).—*Aust. J. Phys.* **6** : 262.
Covington, A. E. (1949).—*Proc. Inst. Radio Engrs., N.Y.* **37** : 407.
Denisse, J. F., Blum, E. J., and Steinberg, J. L. (1952).—*Nature* **170** : 191.
van de Hulst, H. C. (1949).—*Nature* **163** : 24.
O'Brien, P. A. (1953).—*Mon. Not. R. Astr. Soc.* **113** : 597.
Piddington, J. H. (1954).—*Astrophys. J.* **119** : 531.
Piddington, J. H., and Davies, R. D. (1953).—*Nature* **171** : 692.